Mario Ries
Imaging Division
Radiotherapy
Tel +31 88 75 50272
Fax +31 88 7555850
M.G.Ries@umcutrecht.nl

University Medical Center Utrecht

December 28th, 2012

Matthew Eames, Ph.D.
Director of Extramural Research
Focused Ultrasound Foundation
1230 Cedars Ct, Suite F
Charlottesville, VA 22903

Dear Dr. Eames,

since our research project with the title “Heterogeneity correction for improved breast cancer ablation” has been completed for some time, here is the final report which summarizes the progress and achieved results.

Introduction:

This research project was based on the following hypothesis: The risk of undesired tissue damage to thoracic cage, heart and lung during MR guided HIFU ablations of breast tumors can be greatly reduced if a phased array transducer design with a lateral beam direction is used in combination with a large aperture. However, such designs are intrinsically more susceptible to focus aberrations due to heterogeneous tissue within the beam path.
The hypothesis of the research project was, that it would be possible to correct these aberrations by combining high resolution MRI measurements of the tissue distribution with acoustic simulations of the propagation path. The anticipated work of the project included the implementation of the correction strategy and the experimental validation of this compensation strategy with both acoustic simulations and pressure measurements on breast-tissue mimicking ablation phantoms. Due to the limited funding, clinical work was not planned in the scope of this study, however, it was anticipated that this preliminary technical work would contribute to subsequent clinical study on breast cancer therapy with MR-guided HIFU.

Anticipated research program:

The declared Milestones of the original grant application can be summarized to the following six major points:

1. Integration of a prototype wide aperture transducer in a clinical breast platform.

2. Adaptation of a detachable hydrophone set-up allowing 3D acoustic pressure measurements.

3. Characterization of the focal point in a homogenous medium and in a breast mimicking phantom. For the later in particular the dephasing and the intensity attenuation is of particular importance.

4. Implementation of a phase and amplitude correction based on direct acoustic measurements of all contributing transducer channels.

5. Combination of acoustic celerity measurements with segmented high resolution MR-images images in order to obtain the same phase correction information based on the MR images.

6. Comparison of direct (acoustic) and indirect (MR-based) phase and amplitude corrections.

Mario Ries
Imaging Division
Radiotherapy
Tel +31 88 75 50272
Fax +31 88 7555850
M.G.Ries@umcutrecht.nl

The anticipated start of the project was February 1st 2011 for the duration of one year. However, it became increasingly clear that the original research team located in Bordeaux, France (IMF, FRE 3313 CNRS/University Victor Segalen Bordeaux 2) would in the near future relocate to Utrecht, The Netherlands. Since this would in all likelihood result in an interruption of the research activities during 2011, the team decided after consultation with the FUS-Foundation to modify the research plan in order to accommodate this organizational difficulty: The initial tasks were to be started as early as possible, even before the official funding period, in order to gain some headway in the anticipated project. Furthermore, since the IMF laboratory in Bordeaux was only indirectly attached to the university hospitals in Bordeaux, the original research plan did not include tests on human tissue samples. Since the new research location at the UMC Utrecht had the possibility to obtain breast samples from the pathology department, additional experiments on pathological samples were added to the research plan:

7. Comparison of direct (acoustic) and indirect (MR-based) phase and amplitude corrections on human breast tissue.

Mario Ries
Imaging Division
Radiotherapy
Tel +31 88 75 50272
Fax +31 88 7555850
M.G.Ries@umcutrecht.nl

University Medical Center Utrecht

Progress of the work:

Task 1: Integration of a wide aperture transducer in a clinical breast platform (November 2010 to February 2011)

In the original grant application (written mid 2010) we anticipated to use an in-house build 256-channel prototype transducer system, which was designed for preclinical experimentation (proof of concept) of breast cancer ablation. The main innovation of this system was a laterally firing transducer with a large aperture-to-focal length ratio. The initial Milestone of the FUS-foundation project included the integration of this transducer into an experimental testbed. It turned out that in September 2010 Philips Healthcare finished the assembly of their first (pre-) clinical prototype of new Sonalleve breast ablation system. The design of this Sonalleve platform was with respect to these two principal innovations even further optimized than our in-house system. Since Philips Healthcare had committed to support this grant initiative with respect to platform integration, their suggestion was to leapfrog the initial in-house devised design and to conduct the anticipated work directly on a more refined platform, which was also suitable for subsequent clinical usage. In the final agreement, Philips Healthcare made this Sonalleve prototype available for the duration of the project in form of a loan. The Sonalleve platform was shipped in November 2010 to Bordeaux and became two months later operational for preclinical work.

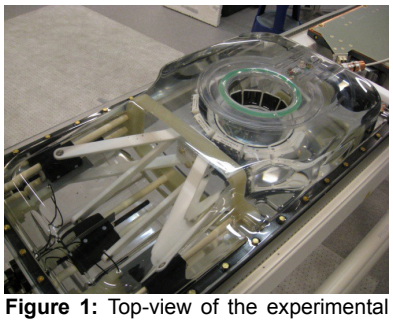

Figure 1: Top-view of the experimental Sonalleve breast HIFU system that Philips healthcare made available for the grant project. The composite transducer consists of eight petal shaped transducer elements in a circular arrangement. This leads to a very high aperture of the system.

Task2: Adaptation of a detachable hydrophone set-up (February 2011 to August 2011)

In order to conduct 3D measurements of the acoustic pressure in and around the focal point of the breast platform, the in-house developed hydrophone measurement platform needed to be adapted: The system consisted of two major components: The mechanical platform and the acquisition electronics. The mechanical platform consists of a modular scaffolding of aluminum bars (25 mm structural elements sourced from Thor labs), which carried three linear M ILS-150PP stages (Newport, Irvine, California,USA) allowing the 3D displacement of the probe hydrophone. The stages were driven with a stepper driver NI-MID-7604 (National Instruments, Austin, Texas, USA), which triggered both the Philips HIFU generator and the acquisition electronics when a new raster point in the 3D measuring grid is reached. The scaffolding and the linear stages were adapted to suit the dimensions of the Sonalleve breast platform. Subsequently, a mechanical coupling mechanism was devised that allowed to dock the scaffolding to the Sonalleve breast platform via a snap-on system. This allows to interleave acoustic and MRI measurements, while the calibrated position is maintained with a high precision. Further adaptations were required for the acquisition electronics: The data acquisition was performed by a 75 µm needle hydrophone (Precision Acoustics, UK) with an integrated 20 dB preamplifier, an intermediate 20dB low-noise amplifier (PR-SA20D, lecoeurelectronique, Chuelles, France) and a PXIe-5122 14-bit digitizer (National instruments, Austin, Texas, U.S.A), which needed to be configured and calibrated to cover the typical acoustic pressure levels of the breast system. Subsequently, a trigger electronic in conjunction with specific sonication protocols had to be devised, which allowed the main Labview acquisition software to remote the Philips HIFU generator.

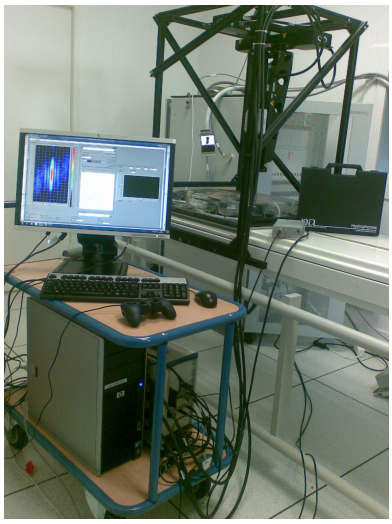

Figure 2: The 3D acoustic pressure measuring system docked to the Sonalleve HIFU table. The docking allows to mount/dismount the the scaffolding within minutes, which allows experiments with interleaved MRI/ acoustical measurements. The scaffolding holds the linear stages, which allow the hydrophone to sample the pressure on a Cartesian grid. The trolley holds the acquisition electronics, the stage driver and the Labview computer.

Mario Ries
Imaging Division
Radiotherapy
Tel +31 88 75 50272
Fax +31 88 7555850
M.G.Ries@umcutrecht.nl

University Medical Center Utrecht

Task 3: Characterization of the focal point in a homogenous medium and in a breast mimicking phantom (February 2011 to August 2011)

In order to perform HIFU interventions on a material composition similar to breast tissue, several polymer materials were evaluated with respect to their celerity and attenuation to represent adipose tissue (1451 ± 36 m/s) and glandular breast tissue (1538 ± 22 m/s). Parallel to the sourcing of a variety of different polymer materials for testing, a fast way to measure the material celerity was implemented. The approach was based on straight-line propagation delay measurements across the different media. For this, a sample of each material was filled in a cylindrical measurement cell of 5cm length. Subsequently, the phase-shift of an ultrasonic pulse of 20 cycles was compared to the values obtained in demineralized and degassed water, which served as a reference. The celerity difference is seen as the phase shift between the pulses. The measurement setup used the acquisition system of the hydrophone setup with am additional piezoceramic piston transducer (Imasonic, Voray sur l'Ognon, France) with a diameter of 5.8 mm and center frequency of 1.45 MHz, which was driven directly by an PXI-5412 (National instruments, Austin, Texas, U.S.A) arbitrary waveform generator.

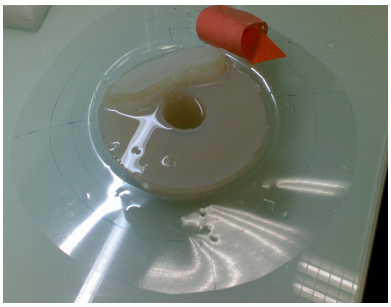

Figure 3: Mold form for the fabrication of the breast phantom with the cast phantom. Visible is mainly the agar gel matrix, with a larger chunk of the embedded TTP1 polymer blocks vsible on the top. Note the centered well hole that allows hydrophone measurements.

The most promising design for this purpose was a two-component phantom consisting of a 3% agar-gel matrix (celerity 1485 m/s and attenuation 1.4 Np/m at 1.45 MHz) and embedded blocks of Model TTP1 polymer material (ATS laboratories Inc., Bridgeport, CT, celerity 1528 m/s and attenuation 8 Np/m at 1.45 MHz). The phantom contained a central conic recess that was filled with degassed water to allow displacement of the hydrophone needle for 3D acoustic field mapping. For the experiments which characterize the heating efficiency, the central aqueous conic part was replaced with 3% agar + 3% silica gel matrix in order to absorb the ultrasound wave at the focal point location. The focal point (i.e. the three dimensional acoustic pressure distribution in the geometric center of the transducer) was systematically mapped for different transducer positions and electronic beam deflections. Subsequently, the influence of the aberration media on the focal point shape was tested for several configurations and the phase shifts of the individual transducer elements evaluated.

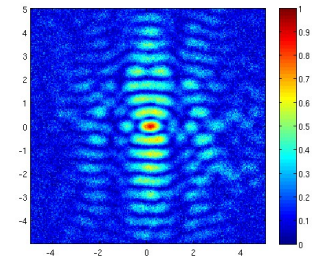

Figure 4: Example of the pressure measurements obtained with the hydrophone measurement platform. Shown is a 2D subset of the full 3D scan of the pressure distribution of the focal area.

Task 4: Implementation of a hydrophone based phase and amplitude correction (February 2011 to August 2011)

In order to measure the the influence of an aberration media on the individual attenuation and dephasing of the individual transducer elements at the natural focus of the transducer an effective (i.e. accurate and reasonably fast) way to center the hydrophone in the focus had to be implemented. For this, the sonication phantom was removed and replaced by degassed and demineralized water to provide a uniform celerity between each transducer channel and the hydrophone needle. When a single transducer channel is used as the signal source, the pulse delay measured by the hydrophone is proportional to the distance from the head of the needle to the center of this element. The known celerity of the degassed water multiplied by the delay provides a distance measurement for each transducer element. The resulting 256 distances allow an accurate quantification of the hydrophone head localization in 3D space relative to the geometric center of the transducer. This

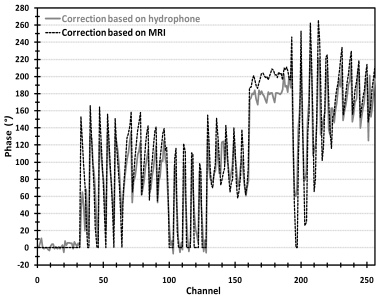

Figure 5: Measurement of the relative phase shift between the 256 transducer elements, when the transducer fires through the heterogeneous breast mimicking phantom. Both the hydrophone derived correction (black) and the MRI based correction (grey, see Task 5) are shown.

Mario Ries
Imaging Division
Radiotherapy
Tel +31 88 75 50272
Fax +31 88 7555850
M.G.Ries@umcutrecht.nl

triangulation procedure was implemented in an automated iterative procedure in LABVIEW, which allowed a precise positioning in under one minute. Once in position, an automated measuring routine obtained the phase and amplitude difference of each individual channel in about ten minutes. Subsequently, the measurement can be repeated with the aberration media in place to evaluate the relative difference compared to the reference experiment conducted in water only. As a proof of principle, the complex conjugate of the evaluated phases are transferred to the HIFU generator and serve as an aperture correction function. The effect of this measure should be a reconstitution of the original unaberrated focal point shape, which was confirmed with 3D pressure mapping.

Task 5: Combination of acoustic celerity measurements with segmented high resolution MR-images images in order to obtain the same phase correction information based on the MR images (February 2011 to August 2011)

For this approach high-resolution MRI images (3D T2-weighted gradient recalled fast field echo with a resolution of 0.8x0.8x0.9mm^3) were used to create a 3D description of the adipose tissue compartments within the HIFU beam path. Combined with celerity and attenuation measurements of the polymer materials described in the previous paragraph, this allows to perform a simulation of the acoustic propagation of the waves from each individual transducer element and to estimate the resulting phase differences and amplitude losses in the targeted focal spot. These theoretical predictions of the amplitude loss and the dephasing are applied as corrections on the HIFU system during the actual ablation process. Subsequently, the results have been validated by direct 3D measurements of the acoustic pressure distribution.

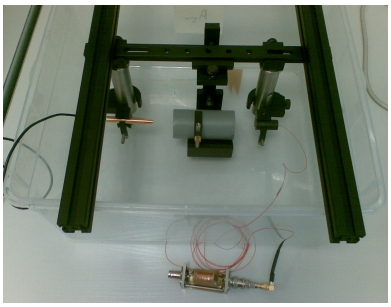

Figure 6: Setup for the celerity and attenuation measurements. The central cylinder holds the sample, while a piezoelectric transducer (right) emits the soundwave, which is detected by the hydrophone (right). The measurement is conducted submerged in demineralized water, both with the sample present and removed. The relative difference of the time-of-arrival and the amplitude of the transmitted acoustic wave allows to obtain both attenuation and celerity of the sample.

Task 6: Comparison of direct (acoustic) and indirect (MR-based) phase and amplitude corrections (February 2011 to August 2011)

The anticipated conclusion of the grant project was a direct comparison of the hydrophone based phase and amplitude correction (task 5) and the MRI based based phase and amplitude correction (task 6). The most challenging aspect of this experiment was to maintain the calibration of the hydrophone setup (in particular the reference position with respect to the natural focus of the transducer) before and after the MR-measurements, since the scaffolding had to be temporarily removed. The findings of this experiment confirmed the initial hypothesis, that the degrading effects of an inhomogeneous propagation media (similar to breast tissue) on the focal point shape can be significantly reduced by a non-invasive MRI based correction strategy.

As a result, the preliminary results of this comparison and the effects of the phase and amplitude aberration have been reported during the *annual meeting 2011 of the International Society for Therapeutic Ultrasound (ISTU)* under the title “MRI based Heterogeneity Correction for Large Aperture HIFU Transducers”. A more refined analysis of the experiments was subsequently published in *Medical Physics* under the title “High intensity focused ultrasound with large aperture transducers: a MRI based focal point correction for tissue heterogeneity.”

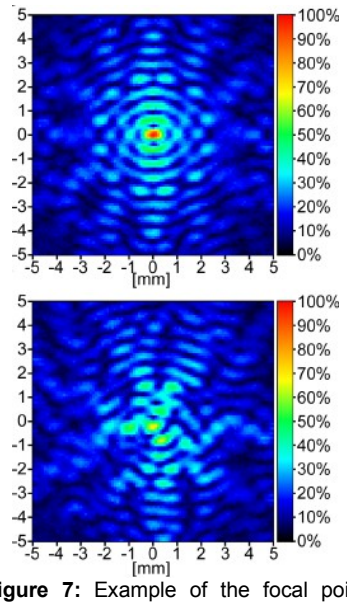

Figure 7: Example of the focal point shape without corrections (bottom) and with MRI-based corrections applied. Details of this experiment can be found in the appendix of the report.

Mario Ries
Imaging Division
Radiotherapy
Tel +31 88 75 50272
Fax +31 88 7555850
M.G.Ries@umcutrecht.nl

University Medical Center Utrecht

Task 7: Comparison of direct (acoustic) and indirect (MR-based) phase and amplitude corrections on human breast tissue samples (December 2011 to March 2012)

For these experiments three human breast tissue sample were collected from the pathology department of the UMC Utrecht. For the experiments the samples were placed asymmetrically in the Philips Sonalleve breast system. Of particular interest was the maximum dephasing and attenuation of the transducer elements when an asymmetric position is ablated. The required hydrophone measurements required to create a lateral water filled recess using a mylar film separation, which allowed free movement of the hydrophone needle. Furthermore, the employed MRI sequences had to be adapted to allow a segmentation of the breast tissue and a volumetric representation of the aberration medium in spatial high-resolution. In this case a high-resolution T2- weighted gradient recalled fast field echo with a resolution of 0.8x0.8x0.9mm^3 was employed for this purpose. Combined with celerity measurements on the pathological samples (adipose and glandular tissue), this allowed to perform a simulation of the acoustic propagation of the waves from each individual transducer element and to estimate the resulting phase differences and amplitude losses in the targeted focal spot. The subsequent comparison of this correction approach with a correction based on direct acoustic measurements concluded the validation of the initial hypothesis of the research project.
The findings conclusions of these experiments have been presented during the 2012 Symposium of the FUS-Foundation in Bethesda, USA and can be found in more elaborate detail detail in the appendix.

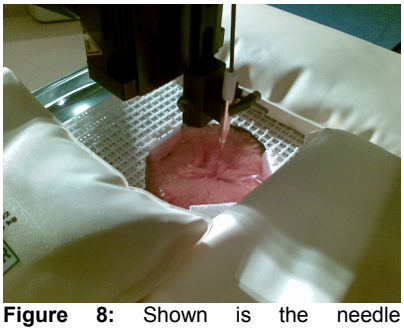

Figure 8: Shown is the needle hydrophone, which is mounted on the motorized scaffolding, while obtaining a pressure map above a human breast sample.

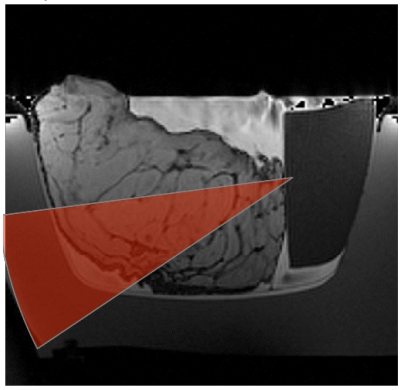

Figure 9: High resolution MRI of the experiment shown in figure 8. The bright tissue represents adipose tissue layers, while the dark tissue structure represents the remaining glandular tissue (since the donor was of high age, few glandular structure remain). The mylar compartment on the right side allos to map the focal point of the HIFU system for asymmetric shot configurations.

Mario Ries
Imaging Division
Radiotherapy
Tel +31 88 75 50272
Fax +31 88 7555850
M.G.Ries@umcutrecht.nl

University Medical Center Utrecht

Outcome and contribution to the Foundation's goals

The obtained results contributed significantly to the understanding of phase and amplitude aberrations, which can occur when human breast tissue is treated with HIFU transducer designs of large aperture and their associated correction strategies. Many of the learned lessons contributed to mature the prototype of the Philips Sonalleve breast platform to the point where a clinical trial could be envisioned. In particular, a simplified version (location dependent pre-tabled correction for phase and amplitude) of the researched aberration correction approach was implemented for clinical evaluation in the platform firmware.

This clinical evaluation is currently conducted at the UMC Utrecht in the scope of a larger CTMM (Center for Translational Molecular Medicine, The Netherlands) funded project (Project title: Non-invasive treatment of cancer by MRI-guided high-intensity focused ultrasound ablation; Project acronym : VOLTA; Project number: 05T-201).

Furthermore, the results and experiences have been made available to the research community by the following publications and conference contributions, which are added as an appendix to this document:

Publications:

Mougenot C, Tillander M, Koskela J, Köhler MO, Moonen C, Ries M. *High intensity focused ultrasound with large aperture transducers: a MRI based focal point correction for tissue heterogeneity.* Med Phys. 2012 Apr;39(4):1936-45.

Conference contributions :

Mougenot C, Tillander M, Koskela J, Köhler MO, Moonen C, Ries M. *MRI based heterogeneity correction for large aperture HIFU transducer.* Proceedings of the 2011 meeting of the International Society for Therapeutic Ultrasound (**ISTU**) in New York, USA

Ries M, Köhler MO, Koskela J, Tillander M, Moonen C. *MRI based heterogeneity correction for large aperture HIFU transducer.* Proceedings of the 2012 Focused Ultrasound Foundation Symposium in Bethesda, USA

Finally, please let me express on behalf of the University Medical Center Utrecht and our HIFU team our gratitude for the generous support for this research project. Since this financial contribution allowed to conduct essential preclinical work, which helped to facilitate clinical trials for HIFU breast cancer treatment, we hope that the FUS-Foundation is satisfied with the outcome of the conducted work.

Please feel free to contact me for any additional questions.

Sincerely,

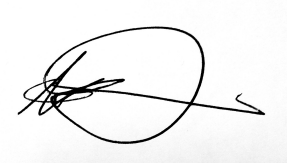

Mario Ries, PhD

Assistant professor Image Sciences Institute

University Medical Center Utrecht, The Netherlands

MRI based Heterogeneity Correction for Large Aperture HIFU Transducers

Charles Mougenot[1], Julius Koskela[1], Matti Tillander[1], Max Köhler[1], Chrit Moonen[2] and Mario Ries[2]

[1]Philips Medical Systems, Finland, [2]Laboratory for Molecular and Functional Imaging, Bordeaux, France

Introduction

The risk of undesired tissue damage to thoracic cage, heart and lung during MR guided HIFU ablations of breast tumors can be greatly reduced if a phased array transducer design with a lateral beam direction is used in combination with a large aperture [1,2]. However, such designs are intrinsically more susceptible to focus aberrations due to heterogeneous tissue within the beam path. The presented work proposes a compensation for these focus aberrations by combining high resolution MRI measurements of the tissue distribution with acoustic simulations of the propagation path. The result is a phase correction for each individual transducer element, allowing to reestablish the original form of the focal point.

Materials and Methods

The proposed approach uses high-resolution MRI images (in the presented example a 3D TSE sequence with TR=1s, TE=80ms, TSE factor=30, α=90°, resolution 1×1×2mm as shown in figure 1A) to create a 3D description of the different tissue compartments within the HIFU beam path. The knowledge of the tissue composition is combined with independent measurements of the speed of sound for each tissue type, to calculate a 3D representation of the celerity distribution in the target object. This allows to perform a simulation of the acoustic propagation of the waves from each individual transducer element and to estimate the resulting phase differences in the targeted focal spot. These are applied as corrections on the HIFU system during the actual ablation process. The feasibility of the method was investigated using a breast phantom consisting of an agar gel matrix (3% agar, celerity 1487 m/s attenuation 0 Np/m) with embedded polymer blocks (celerity 1530 m/s attenuation 10 Np/m) representing the acoustic properties typically encountered in human breast tissue (fatty/glandular [3]). The phase corrections were calculated for a dedicated Sonalleve breast HIFU system (Philips Healthcare, Vantaa, Finland) which uses a large aperture transducer system (240° opening angle, focal length 13cm) composed of 256 channels working at 1.45MHz. The HIFU system is integrated into the patient bed of the 1.5T Philips Achieva system used for MR-imaging. The effectiveness of the proposed correction method was evaluated through direct 3D acoustic pressure measurements in the focal point area and compared to an invasive reference method, which is based on reversing the direct acoustic phase measurements of each transducer channel at focal point.

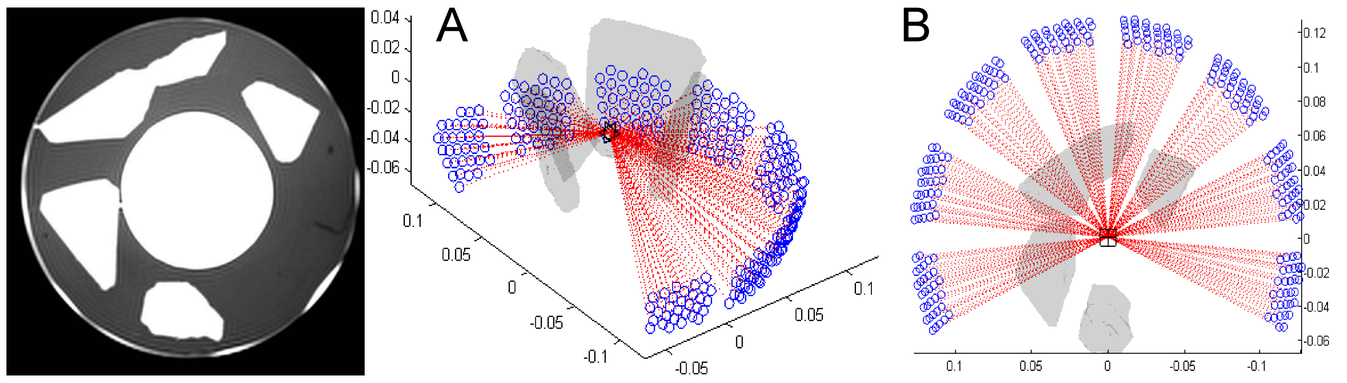

Figure 1:Coronal view of the 3D volumetric MRI which serves as a basis for a 3D model of the tissue celerity. The model is injected in a 3D simulation of the acoustic beam path (A,B). The resulting correction is used to optimize the focal point shape by compensating phase differences.

Results and Discussion

Figure 2 presents the acoustic pressure distribution in a homogenous media (Fig 2A) and in a heterogeneous media (B,C,D). The reference experiment (Fig 2B) uses a phase correction based on direct phase measurements using a hydrophone at the location of the natural focus. In direct comparison the proposed phase correction based on MRI data (Fig 2C) shows a comparable focus quality. Finally, the pressure distribution in a heterogeneous media in absence of any phase correction (Fig 2D) displays the significant loss of focus quality and peak pressure amplitude: The focal point is split into two lobes and the peak pressure is reduced to 69.6% of the value obtained when using the invasive reference method for correction. In comparison, the non-invasive MRI based phase correction also allows to reestablish the original focal point shape and to regain 94.6% of the maximal achievable pressure amplitude.

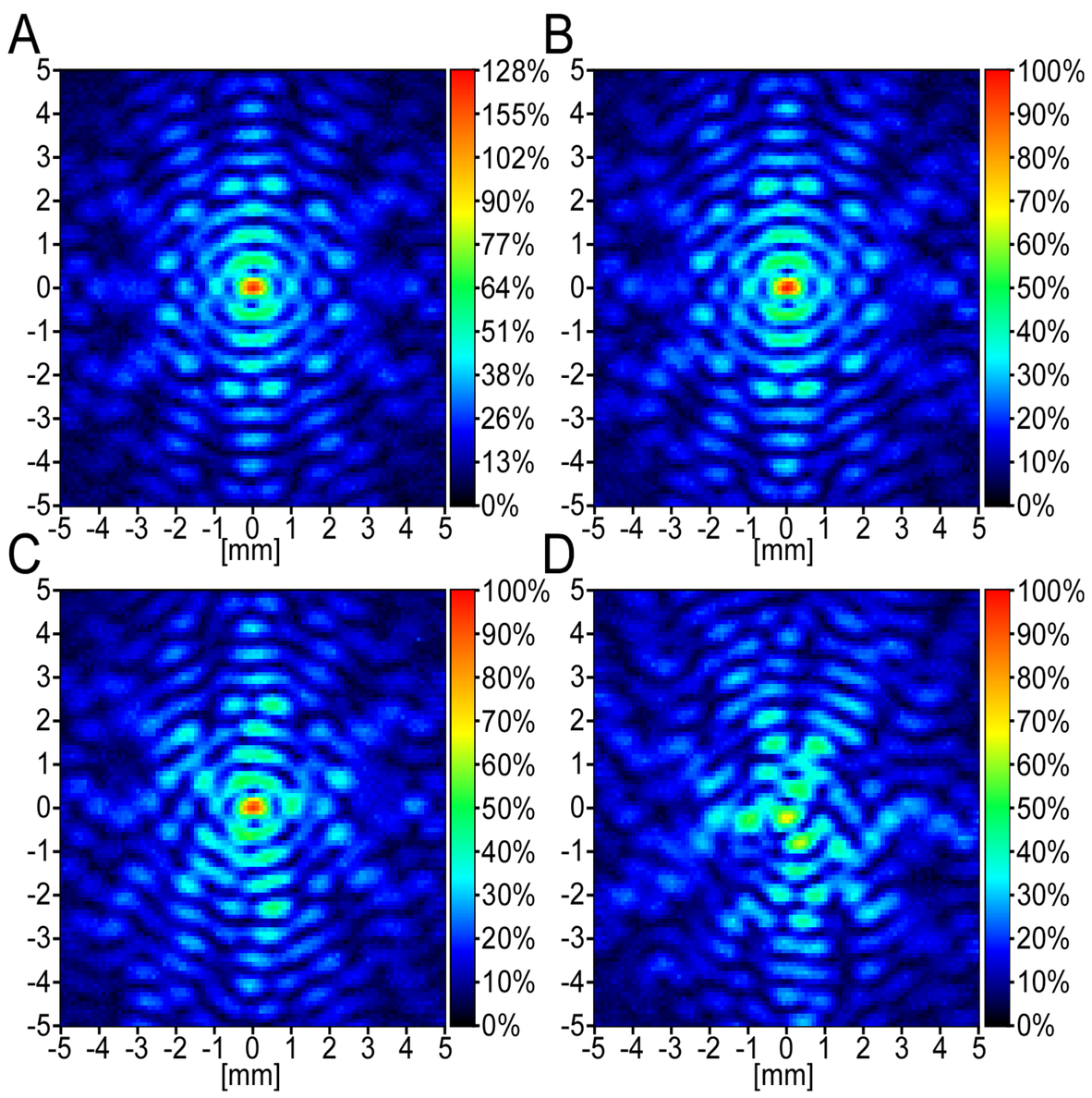

Figure 2: The measured normalized pressure distribution in the focal plane for a homogeneous propagation media (water) for comparison and in a heterogeneous media (B, C, D). The result of figure (B) is obtained when a phase correction based on direct hydrophone measurements are used and serves as a reference. The pressure distribution shown in figure (C) is the result of a phase correction obtained from MRI-data, which is due to its non-invasive nature compatible compatible with clinical application scenarios. Note the good correspondence of both approaches (B,C). Finally, the pressure distribution obtained in absence of any phase correction shown in figure (D), dispays the loss in in amplitude and focus due to the aberrator.

Conclusion

Although the effectiveness of the proposed correction method is in practice limited by the spatial resolution of the MR images and the accuracy of the tissue celerity quantification, the presented first experiments under realistic conditions showed very encouraging results: An optimal focal point shape allows to increase ablation efficiency and to reduce the risk of undesired tissue damage in adjacent areas. The proposed method is non-invasive and compatible with a standard interventional pre-planning and thus a step towards optimal treatment efficiency of MR-guided HIFU ablations in heterogeneous tissues such as the human breast. Future work includes an analysis of the required MR-resolution and accuracy of the tissue celerity on biological tissue samples.

References

[1] Moonen CTW et al. Berlin: Springer; 2006. p 183-2000.

[2] C. Mougenot et al., Large Aperture Transducer Designed for MR-HIFU Treatment of Breast Tumors. ISTU 2011

[3] Scherzinger AL et al. Ultrasound Med Biol. 1989;15(1): 21-8.

Acknowledgments: This project received financial support of the FUS-Foundation.

MRI based Heterogeneity Correction for Large Aperture HIFU Transducers

Mario Ries[1], Max Köhler[2], Julius Koskela[2], Matti Tillander[2], Chrit Moonen[1]

[1]Image Sciences Institute, University Medical Center Utrecht, The Netherlands, [2]Philips Medical Systems, Finland

Introduction

The risk of undesired tissue damage to thoracic cage, heart and lung during MR guided HIFU ablations of breast tumors can be greatly reduced if a phased array transducer design with a lateral beam direction is used in combination with a large aperture [1,2]. However, such designs are intrinsically
more susceptible to focus aberrations due to heterogeneous tissue within the beam path. Recently, a compensation for these focus aberrations by combining high resolution MRI measurements of the tissue distribution with acoustic simulations of the propagation path has been suggested [3]. The result is a phase and amplitude correction for each individual transducer element, allowing to reestablish the original form of the focal point and the pressure amplitude.
The presented work validates this compensation strategy with both acoustic simulations and pressure measurements on human breast-tissue samples.

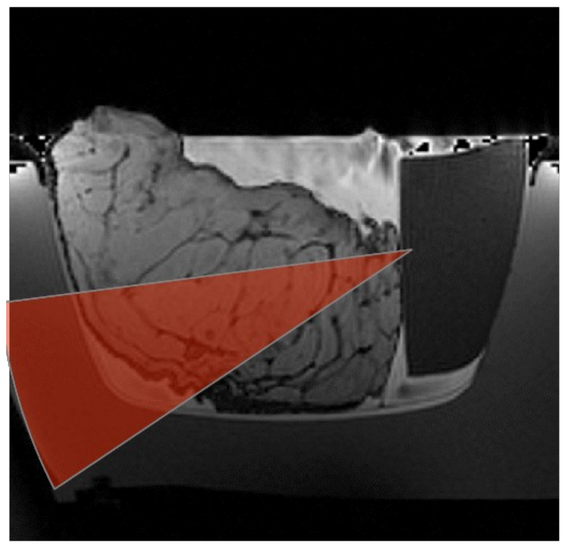

1) High-Resolution MRI depicting the location of the transducer and thetarget area.

Materials and Methods

A human breast tissue sample was placed asymmetrically in a Philips Sonalleve breast HIFU-ablation system (Philips, Vantaa, Finnland), which is integrated in a clinical 1.5T Philips Achieva MRI (Philips,
Best, The Netherlands). In order to evaluate the maximum dephasing of the transducer elements due to
different propagation paths to the ablation area, a lateral water filled recess was created using a mylar film separation, as shown in figure a). High-resolution MRI images (3D T2-weighted gradient recalled fast field echo with a resolution of $0.8\times0.8\times0.9mm^3$) were used to create a 3D description of the adipose tissue compartments within the HIFU beam path. Combined with celerity measurements similar to [3], this allows to perform a simulation of the acoustic propagation of the waves from each individual transducer element and to estimate the resulting phase differences and amplitude losses in the targeted focal spot. These are applied as corrections on the HIFU system during the actual ablation process. The results have been validated by direct acoustic measurements.

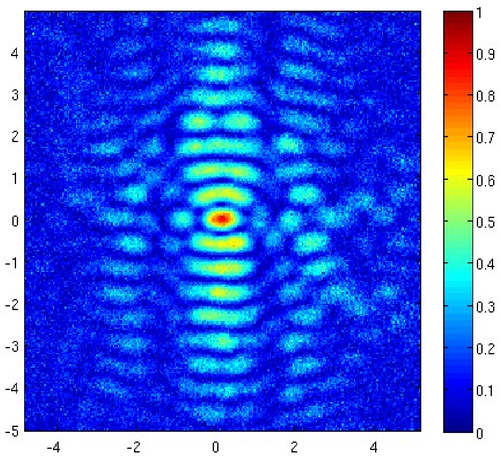

2) Pressure distribution in absence of any correction.

Results

Figure 2) shows the pressure distribution of the focal point area in coronal direction if no aperture corrections are applied. Compared to an unobstructed sonication (not shown), the peak beam pressure is reduced by 50%. Although a simply two-fold power compensation can reestablish the original pressure amplitude, the focal point area (FWHM) increases from initially 0.5x0.5mm2 to 1.2x3.1mm2. In comparison, a matching phase and amplitude correction based on acoustic simulations as shown in figure d) leads to the same peak pressure intensity, while maintaining the original focal point shape.

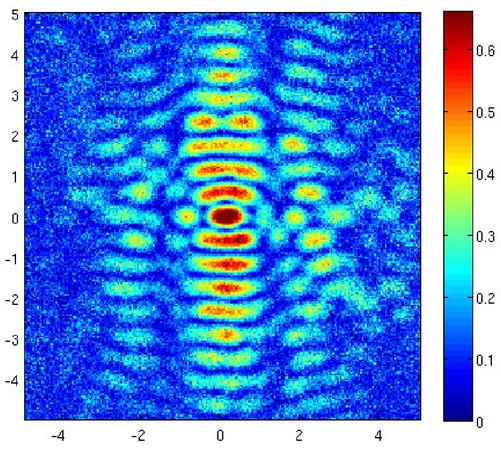

3)Pressure distribution with bulk power compensation.

Discussion

Although the effectiveness of the proposed correction method is in practice limited by the spatial resolution of the MR images and the accuracy of the tissue celerity quantification, the presented first experiments under realistic conditions showed very encouraging results: An optimal focal point shape allows to increase ablation efficiency and to reduce the risk of undesired tissue damage in adjacent areas. The proposed method is non-invasive and compatible with a standard interventional pre-planning and thus a step towards optimal treatment efficiency of MR-guided HIFU ablations in heterogeneous tissues such as the human breast. Future work includes an analysis of the required MR-resolution and accuracy of the tissue celerity on biological tissue samples.

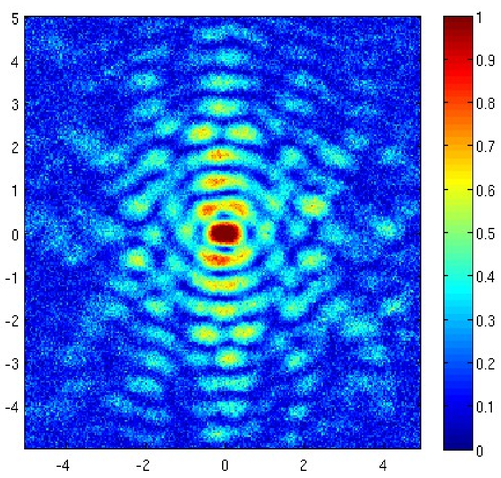

4) Pressure distribution with matched phase and amplitude correction.

References

[1] Moonen CTW et al. Berlin: Springer; 2006. p 183-2000.
[2] C. Mougenot et al., Large Aperture Transducer Designed for MR-HIFU Treatment of Breast Tumors. ISTU 2011
[3] Mougenot C,et al. Med Phys. 2012 Apr;39(4):1936-45.

Acknowledgments: This project received financial support of the FUS-Foundation.

High intensity focused ultrasound with large aperture transducers: A MRI based focal point correction for tissue heterogeneity

Charles Mougenot[a)]
Philips Healthcare, Toronto L6C 2S3, Canada, and Laboratory for Molecular and Functional Imaging, CNRS/University Bordeaux Segalen, 33000, Bordeaux, France

Matti Tillander, Julius Koskela, and Max O. Köhler
Philips Healthcare, F-01510, Vantaa, Finland

Chrit Moonen and Mario Ries
Laboratory for Molecular and Functional Imaging, CNRS/University Bordeaux Segalen, France, 3300 and Imaging Division, UMC Utrecht, 3584 CX, Utrecht, Netherlands

(Received 24 August 2011; revised 31 January 2012; accepted for publication 20 February 2012; published 19 March 2012)

Purpose: The risk of undesired tissue damage to thoracic cage, heart, and lung during MR guided HIFU ablations of breast cancer can be greatly reduced if a phased array transducer design with a lateral beam direction is used in combination with a large aperture. The disadvantage is an increased sensitivity to focus aberrations due to tissue heterogeneity. Here, the authors propose to restore the focal coherence by using a matched aperture phase correction, which is based on a noninvasively obtained tissue model.
Methods: The method combines high resolution MRI with ultrasound wave measurements of different tissue types to determine a phase correction, which compensates focal point aberrations caused by tissue heterogeneity. 3D segmentation of tissue is used to quantify the relative proportion of each tissue type along a line running from the center of each element of the phased array to the target focal point.
Results: For tissue types with a celerity difference of 3%, the proposed method allows to quantify the phase aberration with an accuracy of $6° \pm 20°$ and a correlation factor $R^2 = 0.95$. Using the refocusing method for a complex heterogeneous phantom resulted in 95% of the maximal pressure, whereas only 70% of the maximal pressure is obtained in absence of any phase correction.
Conclusions: Since the proposed refocusing algorithm is compatible with a standard interventional preplanning and requires only a minimal amount of processing, it presents a promising approach to compensate for aberration in heterogeneous tissues such as the human breast.
[http://dx.doi.org/10.1118/1.3693051]

Key words: high intensity focused ultrasound, MRI, tissue heterogeneity, refocusing

I. INTRODUCTION

The treatment of breast cancer by MR guided HIFU has recently shown great potential to enter clinical practice.[1] However, one of the risks associated to this treatment is the undesired damage of tissue such as the thoracic cage, the heart and the lung, which are located in the far field of the ultrasound beam. An elegant way to circumvent these risks is a phased array transducer design with large aperture and lateral principal beam direction.[2,3] In addition, the lower energy density in the near-field of the beam allows treating larger tumors without exceeding the safety limits for undesired temperature elevations of the subcutaneous tissue layer and the skin.

However, the quality of the focal point of such transducer designs is much more sensitive to the influence of inhomogeneous propagation media due to the large differences in the acoustic path of the individual elements. Breast tissue as an acoustic propagation medium is a complex structure of glandular, fatty, and fibrous tissues, which displays variations of the sound speed of up to 5%.[4,5] The use of such transducer designs may thus result in a poor beam focusing quality that should be corrected for.

The requirement to estimate wavefront aberrations during the propagation of ultrasonic waves across human soft tissue is a well-known problem in the field of diagnostic echography. Initial approaches by Hinkelman *et al.*,[6] Mast *et al.*[7,8] proposed numerical simulations based on models of the acoustic propagation media as a solution. In these approaches, the required 3D model of the local celerity and attenuation has been obtained by either an invasive or even destructive analysis of the sample. Similarly, the requirements of therapeutic transcranial HIFU (Ref. 9) for therapeutic purposes stimulated the development of new HIFU beam aberration correction techniques, such as time reversal mirroring by Thomas *et al.*[10] and a phase correction scheme by Hynynen *et al.*[11] Initially, also these approaches were based on either invasive measurements, or required the physical presence of a strong acoustic reflector in the target area. However, the clinical requirement to perform the characterization of the acoustic

propagation path in a noninvasive way lead rapidly to the use of diagnostic imaging modalities, such as MRI (Ref. 12) and CT (Ref. 13–16) for this purpose. Since MRI has an excellent soft tissue contrast, Salahura *et al.*[17] recently proposed to use high resolution MRI also for the characterization of human breast tissue as the basis for simulations of the ultrasound propagation and the corresponding wavefront aberrations.

However, recent approaches to improve therapeutic HIFU in the human breast tissue by Herbert *et al.*[18] proposed instead to remove beam aberrations by calculating the relative phase shifts between transducer channels from intensity differences in the focus of the beam. The focus intensity was accessed by measuring the radiation force induced tissue displacement with speckle tracking. Hertzberg *et al.*[19] and Larrat *et al.*[20] subsequently refined this approach by substituting the echography based radiation force measurements by their MRI equivalent MR-ARFI. Although both approaches are promising, they are for large transducer arrays time-consuming and challenging to conduct in clinical practice.

Since both water and fat images can be obtained rapidly by MRI, we investigated in this study whether MRI based tissue segmentation similar to the approach of Salahura *et al.*[17] and *a priori* knowledge of the tissue celerity can be combined to a phase correction method, which compensates for focal point aberrations for therapeutic HIFU. Since MR guided HIFU ablations of breast cancer already use MR anatomical images for treatment planning, such a correction method would not require any additional imaging modality and can be integrated in a time effective and seamless way in current therapy protocols.

In order to verify this hypothesis, we devised a complex breast phantom, which mimics the acoustic properties of glandular and fatty tissue and which allows noninvasive beam corrections and HIFU ablations as well as invasive acoustic measurements. This allows in a first step to measure the phase aberrations of the ultrasound beam for each individual transducer element with a high precision hydrophone, which serves subsequently as a gold standard for the noninvasive correction strategy. Subsequently, segmented high resolution MRI images were used to provide a three-dimensional map of the tissue distribution. The combination of this map with the known celerity and attenuation of the tissue represents a three-dimensional description of the acoustic propagation medium. The phase correction for an optimal focal point shape and pressure amplitude is obtained by calculating for each transducer element the relative phase shift, which is accumulated during the acoustic propagation from the emitter through the heterogeneous celerity distribution to the final target zone. In order to render this process compatible with the time constraint of a routine clinical preparation, a fast straight-line approximation of the propagation path was used, which neglects refraction and diffraction effects.

The validity of the resulting noninvasive phase correction approach is experimentally evaluated both by a direct comparison with the invasive hydrophone measurements and by comparing the spatial-temporal evolution of the temperature during HIFU ablation experiments in the presence and the absence of the correction.

Finally, the error introduced by the omission of refraction and diffraction effects on the phase correction is quantified. This is achieved by comparing the results obtained with a straight-line approximation with the results obtained by solving the linear, homogeneous wave equation for a heterogeneous media numerically.

II. MATERIALS AND METHODS

II.A. MR-HIFU platform

The study was conducted with a Philips Sonalleve breast MR-HIFU platform, which is equipped with large aperture phased array transducer consisting of a circular structure surrounding the breast, as illustrated in Fig. 1. The focal length was 13 cm and the operation frequency was 1.45 MHz. Due to manufacturing limitations, the large aperture transducer designs was subdivided in 12 separate modules, each consisting of 32 elements of 6.6 mm diameter. However, for the described study only 246 elements, which were distributed over 8 modules, were used.

A phase calibration of the acoustic signal of each element at the focal point was performed in order to compensate for tolerances in the mechanical assembly of the transducer modules. The phase calibration and focal point shape measurements were performed in degassed water with a hydrophone system described in Sec. II F.

The transducer was integrated in a MR compatible table top including a 3D mechanical positioning system and a dedicated MR breast coil. MRI for the exact measurement of the phantom geometry and MR-thermometry during HIFU sonication experiments for the evaluation of the heating efficiency of each refocusing method were performed inside a clinical Philips Achieva 1.5T scanner. Acoustic field measurements were acquired outside of the MRI room using a hydrophone setup docked on top of this HIFU bed as illustrated Fig. 1(a).

To mimic breast tissue heterogeneity, a two-component phantom consisting of a 3% agar gel matrix (celerity 1485 m/s and attenuation 1.4 Np/m at 1.45 MHz) and embedded blocks of a polymer material (Model TTP1, ATS laboratories, Inc., Bridgeport, CT, celerity 1528 m/s and attenuation 8 Np/m at 1.45 MHz) was manufactured. Both materials were selected to obtain celerities similar to *in vivo* fat (1451 ± 36 m/s) and glandular breast tissues (1538 ± 22 m/s).[21] The phantom contained a central conic recess that was filled with degassed water to allow displacement of the hydrophone needle for 3D-acoustic field mapping. For the experiments which characterize the heating efficiency, the central aqueous conic part was replaced with 3% agar + 3% silica gel matrix (celerity of 1447 m/s and attenuation of 4 Np/m at 1.45 MHz) in order to absorb the ultrasound wave at the focal point location.

II.B. Aberrator segmentation

The proposed approach used high resolution MRI images to create a 3D description of the different tissue compartments within the HIFU beam path. The employed T2-weighted 3D TSE sequence (TR = 1 s, TE = 80 ms, TSE factor = 30,

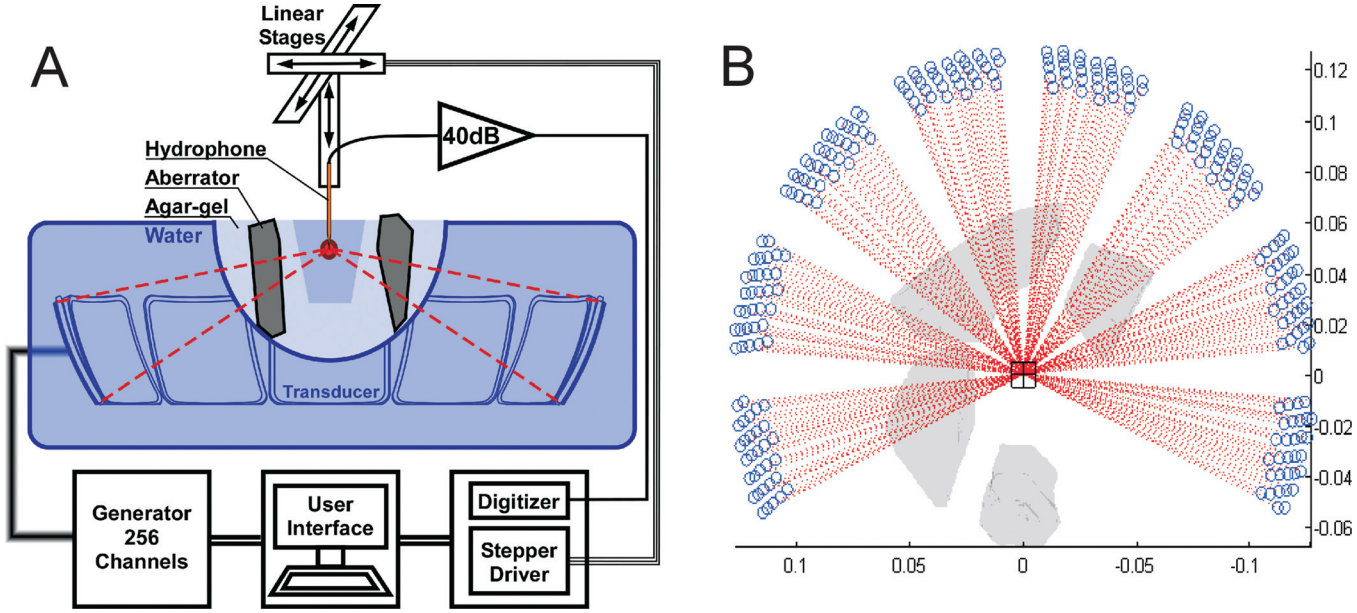

FIG. 1. (a) Block diagram over overview of the breast platform with hydrophone system, (b) top overview of the transducer composed of 256 elements (blue circles) relatively to the aberrators (black transparent blocks). The beam path (red dotted line) across aberrators varies for the different elements resulting in a variation of the phase shifts.

$\alpha = 90°$, resolution $1 \times 1 \times 2$ mm^3, FOV $250 \times 250 \times 128$ mm^3, acquisition time 48 min) was contrast optimized for the three different propagation media.

The acoustic aberrator was segmented from the images with a semi-automatic tool written in IDL (ITT Visual Information Solutions, Boulder, Colorado, USA) on a slice-by-slice basis and subsequently tessalated using a marching cube algorithm.[22] The resulting 3D surfaces were imported into MATLAB (Mathworks, Natick, Massachusetts, USA) for quantification of the corresponding phase correction and simulation of the resulting acoustic field.

II.C. Celerity measurements

In order to calculate the 3D representation of the celerity distribution in the target object, the spatial distribution of the different propagation media needs to be combined with the celerity of each medium.

The required celerity measurements were based on straight-line propagation delay measurements across the different media. For this, a sample of each material was filled in a cylindrical measurement cell of 5 cm length. Subsequently, the phase-shift of an ultrasonic pulse of 20 cycles was compared to the values obtained in demineralized and degassed water, which served as a reference. The celerity difference is seen as the phase shift between the pulses. In addition, the variation of amplitude between the pulses was used to quantify also the attenuation factor of media for simulation purpose only.

The ultrasonic emitter was a piezoceramic piston transducer (Imasonic, Voray sur l'Ognon, France) with a diameter of 5.8 mm and center frequency of 1.45 MHz, which was driven directly by an PXI-5412 (National instruments, Austin, Texas, USA) arbitrary waveform generator. The arrival of the pulses was recorded using a 75 μm needle hydrophone (Precision Acoustics, UK) with an integrated 20 dB preamplifier, an intermediate 20 dB low-noise amplifier (PR-SA20D, lecoeurelectronique, Chuelles, France) and a PXIe-5122 14-bit digitizer (National instruments, Austin, Texas, USA). A dedicated LABVIEW program (National instruments, Austin, Texas, USA) controlled the signal generation, the acquisition, and the subsequent analysis. The pulses were emitted every 5 ms and the measurements averaged over several seconds in order to minimize measurement noise.

II.D. Phase correction

The 3D representation of the celerity distribution was used to quantify the resulting phase shift of the ultrasound waves from each element at the focal point. The phase shift was calculated by assuming straight propagation of the ultrasound waves along a line from the center of each transducer element to the geometric focus as shown in Fig. 1(b). The intersections of each beam path with the different medium layers were used to evaluate the acoustic propagation delay. For this, the resulting phase φ^n of the acoustic wave coming from element n was derived from the linear combination of the time needed to propagate through the different media in the beam path of that element

$$\varphi^n = 2\pi \cdot f \cdot \sum_i \frac{d^i_n}{c^i}, \tag{1}$$

where f is the operating frequency, c^i is the celerity of medium i, and d^i_n the propagation wave distance of the beam path line of the element n across this medium.

This noninvasive phase estimation for each channel was subsequently compared with the phase shift obtained from direct hydrophone measurements at the geometric center of

the transducer. Since the phase quantification strongly depends on the exact position of the hydrophone needle, a triangulation method was used to localize the geometric center of the transducer.

For this, the sonication phantom was removed and replaced by degassed and demineralized water to provide a uniform celerity between each transducer channel and the hydrophone needle.

When a single transducer channel is used as the signal source, the pulse delay measured by the hydrophone is proportional to the distance from the head of the needle to the center of this element. The known celerity of the degassed water multiplied by the delay provides a distance measurement D_n for each transducer element n located in position the $(X_n;Y_n;Z_n)$. The resulting 246 distances allow an accurate quantification of the hydrophone head localization (X;Y;Z) in 3D space relative to the geometric center of the transducer (0;0;0). In practice, it consists of the inversion of the overdetermined linear equation system of the distances D_n as a function of hydrophone needle position (X;Y;Z) described by Eq. (2)

$$\begin{aligned} D_n &= \sqrt{(X - X_n)^2 + (Y - Y_n)^2 + (Z - Z_n)^2} \\ &\cong F - \frac{1}{F}(X \cdot X_n + Y \cdot Y_n + Z \cdot Z_n) \\ \text{with} \quad F &= \sqrt{X_n^2 + Y_n^2 + Z_n^2}. \end{aligned} \tag{2}$$

However, this linear approximation assumes that the hydrophone displacement is small compared to the focal length F of the transducer. This results in a measurement error of 1% if the hydrophone needle is located at a distance of 1 mm from the geometric center of the transducer. To compensate for this approximation, several iterations were used to move the needle toward the exact geometric transducer center. After the focal point position was calibrated, the needle was driven to a parking position, which allowed to insert the acoustic phantom. Subsequently, the hydrophone was repositioned to the calibrated geometric center of the transducer, exploiting the high repositioning precision of the linear stages.

II.E. Acoustic simulation

The experimental results were compared to a numerical simulation of the pressure field in the vicinity of the focal point. This was achieved using an in-house developed stochastic ray tracing method for simulation of acoustic waves. The simulations were performed for an experiment in the presence of the aberration using either the phase correction based on hydrophone measurements, or the phase correction based on MRI data, or without any phase correction. An overview of the ray-tracing method is provided as an Appendix.

In the evaluated simulation set-up, the volume of interest consists of two media: Degassed water and the polymer aberrator, as segmented from MRI data. Layers were characterized by ultrasound velocity c and attenuation α, based on individual measurements as previously described. Within each medium, pressure was assumed to be governed by linear wave equation working in continuous mode at the main harmonic frequency. In the course of the simulations, simulated ray particles, phonons, were generated and propagated from layer to layer, whereby phonons were split into two particles, in order to model reflections. Moreover reflections are assumed to be sufficiently weak, such that multiple reflections can be ignored.

II.F. Focal point characterization

The HIFU focus quality for each aberration correction was evaluated by 3D-mapping of the acoustic pressure field. This was achieved by mapping the pressure point-by-point with a needle hydrophone, which was mounted to three orthogonally oriented linear stages in order to sequentially raster a measurement grid in 3D space.

This setup had two basic components: The mechanical platform and the acquisition electronics. The mechanical platform consists of a modular scaffolding of aluminum bars (25 mm structural elements sourced from Thor labs), which carried three linear M ILS-150PP stages (Newport, Irvine, California, USA) allowing the 3D displacement of the probe hydrophone. The stages were driven with a stepper driver NI-MID-7604 (National Instruments, Austin, Texas, USA), which triggered both the HIFU generator and the acquisition electronics when a new raster point was reached. The scaffolding is docked to the breast platform via a snap-on system to allow to interleave acoustic and MRI measurements. The data acquisition was performed by the same needle hydrophone, amplifier, and NI-PXIe-5122 digitizer setup as used for the celerity measurements described previously.

For measurements of the phase-shift between the acoustic waves of all channels in the geometric focus, the hydrophone needle remained stationary and each of the transducer elements was sequentially measured. The measurement cycle for each element consisted of a pulse of 20 cycles followed by a propagation delay and subsequent signal sampling by the hydrophone. Due to the low acoustic intensity emitted by a single channel, the measurement cycle was repeated 200 times every 10 ms for signal averaging. These sequential phase measurements were also used to triangulate the exact hydrophone needle position as described previously.

II.G. MR-thermometry

The final goal of this study was to experimentally reconfirm the improved heating performance of the refocused HIFU system during an ablation experiment. For that purpose, the central aqueous conic aperture part was replaced by a 3% agar and 3% silica gel matrix (celerity of 1447 m/s and attenuation of 4 Np/m at 1.45 MHz) serving as the ultrasound absorber in the target area. In order to avoid additional dephasing effects from the target absorber gel, the gel matrix composition was matched to result in celerity very close to water and was given in addition a cylindrical shape so that the incoming wave hits the target surface at an angle close to 90°.

To estimate the heating induced by the sonications, referenced proton resonance frequency (PRF) based MR-thermometry was performed on a clinical 1.5 T Philips Achieva MRI, using a spoiled gradient echo sequence with an EPI factor = 11, TE = 20 ms, TR = 36 ms and a flip angle = 20°. A single horizontal slice of 160 × 160 mm with a voxel size of 1 × 1 × 4 mm was acquired every 0.5 s. The reference image was processed by averaging four dynamics prior to the heating in order to increase the SNR. Due to the short monitoring period of 20 s during the heat-up process no additional field drift corrections were used.

To compare the efficiency of the refocusing method, an acoustic power of 100 W was applied to the gel for 5 s at the same location used for all previous experiments. Taking into account the attenuation induced by the agar, the aberrator, and the agar-silica gel, this power level was expected to produce at the center of the focal point an approximate maximal pressure of 4 MPa. Three experiments were performed: One experiment in absence of any phase correction, one experiment with a phase correction based on the invasive hydrophone measurement and one experiment with a phase correction based on the noninvasive MRI based correction method. A cooling period of at least 5 min was used in between each sonication to avoid interactions between the experiments. Each type of sonication was repeated twice for averaging purposes.

III. RESULTS

III.A. Experimental quantification of the phase aberration

As previously described, accurate measurements of the dephasing between the transducer elements at the focal point position require a precise positioning of the hydrophone needle at the geometric center of the transducer. Using the iterative 3D triangulation method in the water filled transducer cavity, this was achievable with a precision of ±10 μm.

Subsequently, the relative phase-shift between the transducer elements was measured in absence of an aberrator with a reproducibility of ±1°. A control measurement of the compensated relative phase differences resulted in a phase distribution centered around 0° with a ±1.6° standard deviation. This remaining standard deviation of the phase values was probably mainly due to the discrete phase step size of 3° of the electrical signals produced.

After the phase calibration, the aberration phantom was inserted in the transducer cavity, and the phase measurements were repeated. As shown by the solid line in Fig. 3, the aberration phantom induced a dephasing of up to 226°. The 32 elements corresponding to the first transducer module were not subject to any significant phase aberration since no polymer aberrator block was located in the corresponding beam path.

III.B. Model based quantification of the phase aberration

The ultrasound propagated from the transducer to the focal point across several media, which are, respectively: water/agar gel/polymer/agar gel/water or agar-silica gel. However, the agar gel and the agar-silica gel had a celerity very close to that of water, and were made with a cylindrical shape leading to a similar medium thickness along the beam path of each element. Thus, the phase aberration induced by those media was considered negligible for this study. As a consequence, only the segmentation of the polymer layer combined with the difference of celerity between the agar gel and the polymer was used to process the phase correction. As shown on MR-image Fig. 2, the T2-weighted sequence offered a good contrast between the agar gel and the polymer. However, ringing artifacts around sharp edges might bias the automatic detection of contours. For this reason, a semi-automatic contouring was used, where the initial contouring done manually is refined by the segmentation tool based on the analysis of the selected edges. A consistent shape of the polymer block was thus obtained from each slice as displayed with 3D rendering in Fig. 2.

The dashed line in Fig. 3 displays the relative phase-shift based on the acoustic propagation model. In this case, a positive phase change of up to 266° was found between the transducer elements. The comparison of the phase shifts derived from the acoustic propagation model and the direct hydrophone measurements resulted in an average offset of 6° and a standard deviation 20°, which is relatively small compared to the amplitude of phase variation.

The phase-shift estimation based the MRI derived acoustic model correlated with the phase-shift measured with the hydrophone with a correlation factor $R^2 = 0.95$. However, the amplitude of phase variations based on the MRI derived acoustic model was on average 14% larger than the phase variations measured by hydrophone.

Further simulation (not presented in this text) indicated that the phase aberration induced by the inclusion of the agar

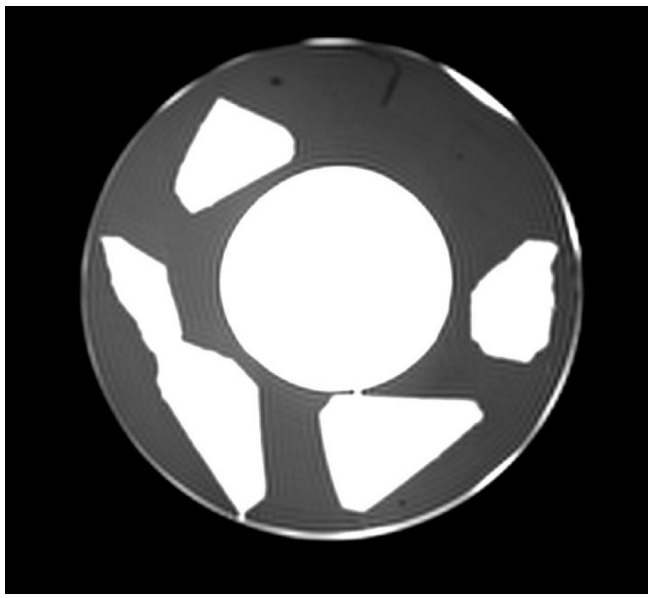

FIG. 2. T2-weighted image of the breast phantom. The native focus of the transducer is in the center of the water filled recess (white circle), the aberrators appear as white triangles. The dark gray structure represents the agar gel matrix.

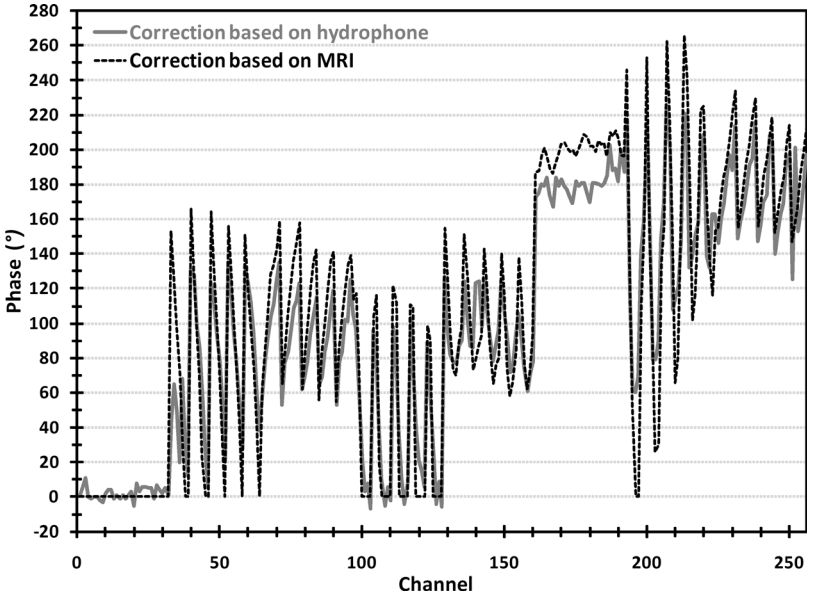

FIG. 3. The graph shows the phase correction based on the line integration method (black dashed line) as compared to the direct acoustic measurement of the phase correction with a hydrophone (solid gray line) for each element.

gel layer in the model corresponds to ±4.6°, which is relatively small compared to the aberration of ±83° induced by the polymer aberrator block. This justifies the use of simpler model of the polymer aberrator block only.

III.C. Pressure distribution

Once the phase aberration was quantified for each element, the achievable refocusing efficiency was quantified with the hydrophone setup by scanning the pressure distribution in three dimensions, with all elements turned on simultaneously. For comparison, the pressure distribution was also obtained from simulations using stochastic acoustic ray tracing method. Figure 4 presents the measured [Figs. 4(a)–4(c)] and simulated [Figs. 4(d)–4(f)] normalized pressure distribution of the resulting focal point in a horizontal slice using the correction based on hydrophone phase measurements [Figs. 4(a) and

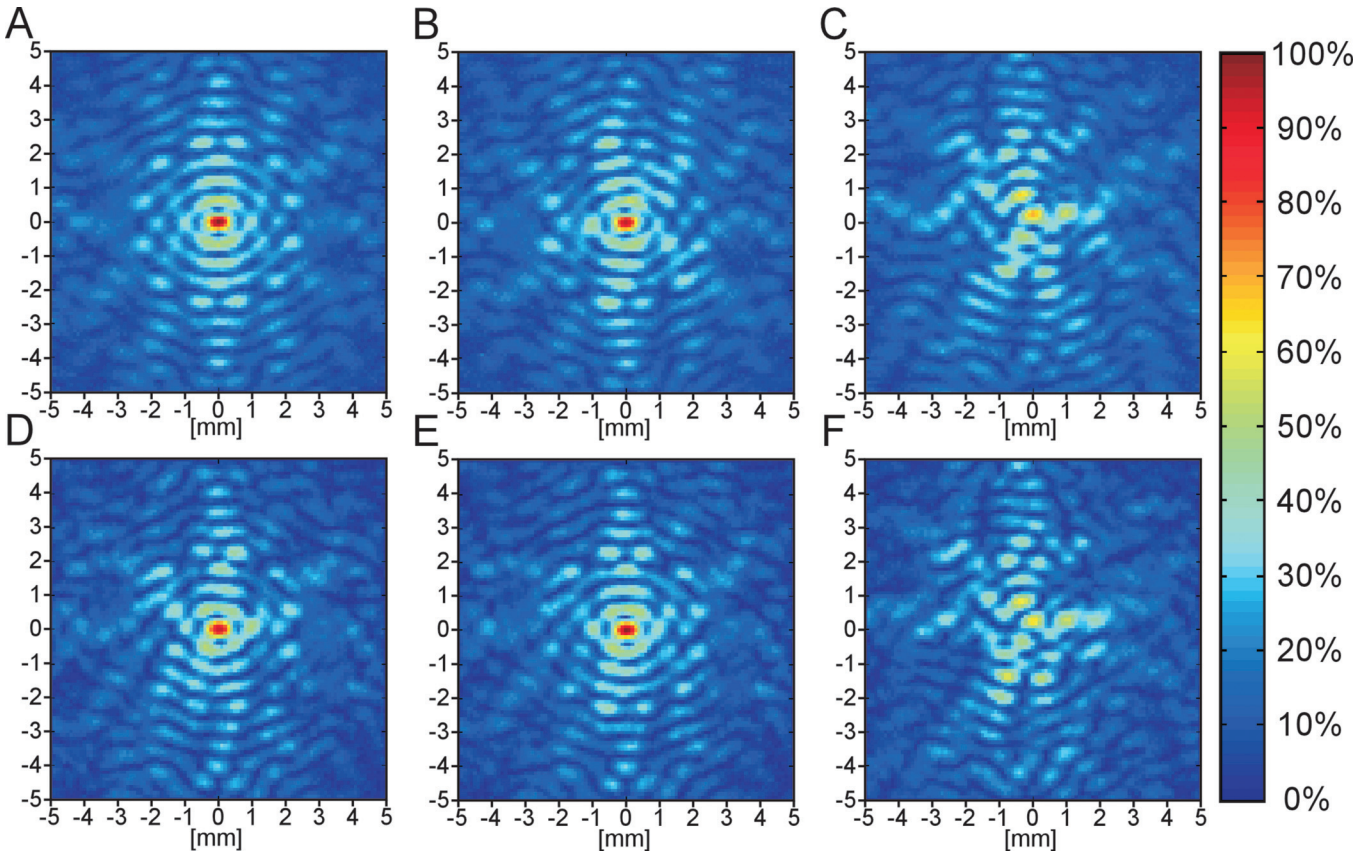

FIG. 4. Normalized pressure amplitude of the focal point (a)–(c) measured with hydrophone scan and (d)–(f) simulated using stochastic acoustic ray tracing method. Comparison is displayed using (a) and (d) correction based on hydrophone phase measurement (b) and (e) correction based on MRI data, and (c) and (f) no phase correction.

4(d)], the correction based on the MRI derived acoustic model [Figs. 4(b) and 4(e)], and in the absence of any phase correction [Figs. 4(c) and 4(f)]. As complementary data, Table I reports the maximal normalized measured or simulated pressure for the same three sonication experiments, as well as the size and volume of the focal point at the threshold of 50% of the normalized pressure. The volume was quantified assuming an ellipsoidal shape of the contour characterized. All experimental pressure measurements were normalized to the maximal pressure (i.e., maximal normalized pressure equal to 100%) obtained with the phase correction based on hydrophone measurements [Fig. 4(a)]. Under the condition that a correction only changes the phase of each transducer element, and not the amplitude, this can be considered to be the maximal pressure achievable within this phantom.

However, since the tissue model used by the acoustic simulations is extracted from the MR images and not based on the actual tissue shape as seen by the hydrophone, the simulated pressures [Figs. 4(d)–4(e)] have been normalized to the maximal pressure level of the model based phase correction (i.e., normalized pressure in Fig. 4(e) equal to 100%).

Despite the difference in normalization, the pressure distribution varied in a similar manner for both the measurements and simulations with the refocusing method used (based on hydrophone or the MRI data). A positive phase delay measured for the refocusing method based on MRI data relatively to the refocusing method based on hydrophone, would correspond to a negative phase delay for the refocusing method based on hydrophone relatively to the refocusing method based on MRI data.

The difference between the maximum pressure obtained when using the hydrophone based phase correction and when using the model based phase correction was + 5% for the measurements or − 6% for the simulations. The negative difference for the simulations comes from the fact that the maximum pressure is obtained when using the model based correction rather than the hydrophone measurements. The difference in focal point volume between the refocusing methods was +9% for the measurements or − 13% for the simulations. The resulting pattern of secondary lobes observed in Figs. 4(b) and 4(e) remains similar to those observed in Figs. 4(a) and 4(d) but some of those lobes have slightly different amplitudes.

The importance of beam refocusing for this aberrator is clearly visible in measurements shown in Fig. 4(c) and simulations in Fig. 4(f). In the absence of any phase correction, the focal point shape is split into two lobes. The more intense main lobe reaches a maximal normalized pressure equal to 70% of the theoretical maximum when directly measured and 64% when simulated. Furthermore, the focal point is shifted 0.2 mm from the geometrical center of the transducer. The volume of this focal point at the 50% threshold of the normalized pressure was reduced by 59% due to the presence of the aberrator according to measurements, and by 84% according to simulations. The pattern of secondary lobes observed in measurements [Fig. 4(c)] and simulations [Fig. 4(f)] was significantly changed with more intense side lobes. Secondary lobes located at the proximity of the main focal point reached a normalized pressure up to 50% which was almost the same normalized pressure as the one in the main focal point.

III.D. Heating efficiency

The improvement of the heating efficiency in the focal point for each correction method was evaluated by performing short 5 s sonications across aberrators and the agar-silica gel under MR-thermometry monitoring. Figure 5 shows a comparison of the temporal [Fig. 5(a)] and the spatial [Fig. 5(b)] profile of the temperature increase, using either a phase correction based on direct hydrophone measurements, or a phase correction based on the MRI derived acoustic model. The temperature profile displayed in Fig. 5 corresponds to the averaging of the temperature rise obtained over the two series of measurements.

The most efficient heating is obtained with the correction based on direct hydrophone measurements, leading to 39.2 ± 2.7 °C temperature increase at the end of the sonication. The use of the correction based on the MRI derived acoustic model results in a temperature rise equal to 34 ± 0.9 °C. For comparison, in absence of any phase correction a temperature rise of 27.7 ± 1.1 °C was measured. The full width at half maximum of the temperature distribution at the end of the sonication was 2.7, 4.2, and 5.4 mm when using correction based on hydrophone, correction based the MRI derived acoustic model and no correction, respectively.

TABLE I. Characterization of the maximum normalized pressure and the focal point size at the threshold of 50% of the normalized pressure based on (upper part) hydrophone measurements and (lower part) simulations using stochastic acoustic ray tracing method, without a phase correction or with a phase correction based on hydrophone phase measurement or MRI segmentation.

			Size at 50% of the normalized pressure			
		Maximal normalized pressure (%)	Length (mm)	Height (mm)	Width (mm)	Volume (mm^3)
Measurements	Phase correction based on hydrophone	100	4.31	0.76	0.43	0.74
	Phase correction based on MRI	94.9	4.13	0.74	0.42	0.68
	No phase correction	69.8	3.18	0.53	0.35	0.31
Simulations	Phase correction based on hydrophone	94.1	4.11	0.73	0.48	0.75
	Phase correction based on MRI	100	4.33	0.77	0.50	0.87
	No phase correction	64.5	2.28	0.41	0.30	0.14

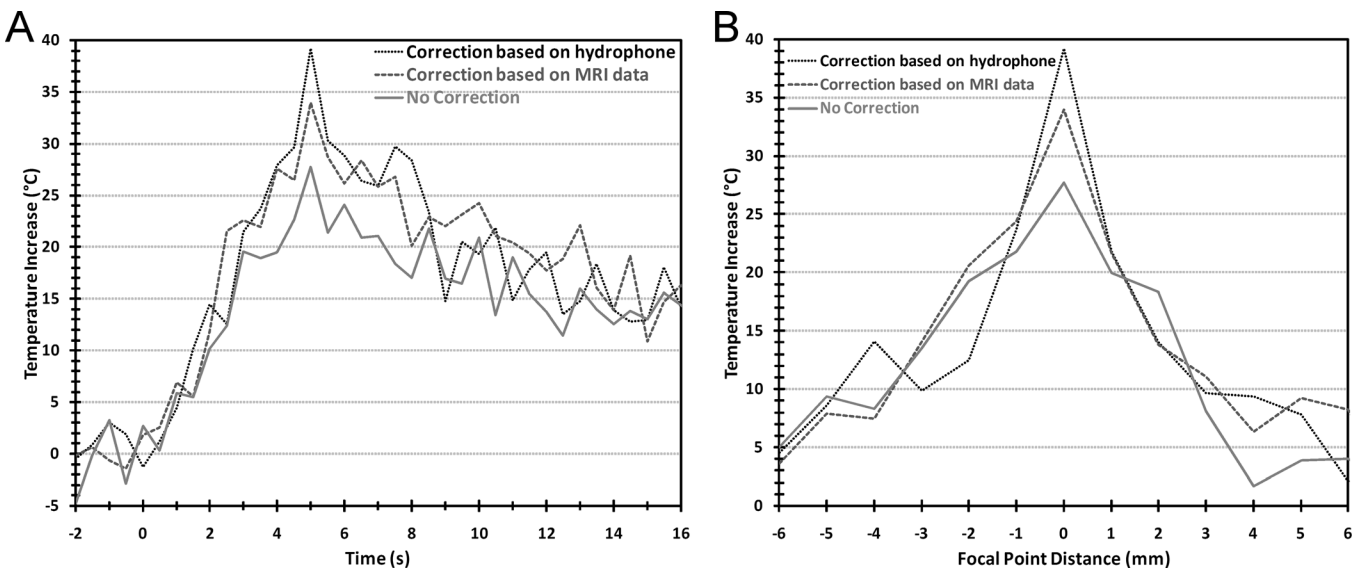

FIG. 5. (a) Temporal profile of the averaged temperature rise measured at the focal point and (b) spatial profile of the averaged temperature rise along a horizontal axis at the end of 100 W 5 s sonication using a correction based on hydrophone (dark dotted line), a correction based on MRI data (dark gray dashed line) or no correction (solid gray line).

IV. DISCUSSION

IV.A. Acoustic model based phase correction

Both the experiments and the simulations showed a clear improvement of the focal point quality when the phase correction based on the MRI derived acoustic model was employed. However, compared to the "gold standard" (hydrophone based corrections) some differences were noted.

These differences can be explained by several contributing factors. For one, the precision of the celerity measurements was generally limited by the uncertainty of the exact sample dimensions, by the imperfections of the sample surface (not perfectly planar and not perfectly parallel) and temperature fluctuations. In practice, the celerity measurement setup provided an accuracy below 1% of the measured celerity value. It should be noted that the celerity measurement is a crucial part of the proposed phase correction method and that an overestimation of the celerity measurement by 0.2% is sufficient to be able to explain the overestimation of the phase correction based on the MRI derived acoustic model.

Another important factor for the limited accuracy of the proposed correction scheme is the chosen resolution of the MRI-datasets. This leads to partial volume effects in the images and thus to tessellation errors of the boundary surface between different tissue types. As a consequence, the thickness of the aberrators might have been overestimated. This would also explain the overestimation of the correction based on MRI data relatively to the phased measured by hydrophone displayed Fig. 3.

Although Salahura *et al.*[17] employed submillimeter resolved MRI for a more precise characterization of the acoustic propagation path, the resolution used for this study was limited to an isotropic resolution of 1 mm. This choice was deliberate, since MR scans with substantially higher resolutions on clinically available whole body MRIs tend to lead to imaging times, which are unfeasible as a routine preparation scan in clinical practice. It should also be noted that the employed lengthy T2 weighted sequence was chosen to facilitate the segmentation of the phantom materials and to avoid image distortions. Instead, most diagnostic MRI protocols for breast cancer already employ T1-weighted gradient recalled MRI with a similar resolution, acquisition times of a few minutes and an excellent contrast between fatty and glandular tissue, and which could potentially be directly used for the proposed correction scheme. However, since the tissue structure of human breast tissue is also substantially more complex than the structure of the employed aberration phantom, the appropriate MRI resolution for an accurate model based phase correction remains to be addressed in future studies.

Finally, the use of a line integration method from the center of the element to the focal point center, as described in Eq. (1), might also be a too simple approximation. The ultrasound wave at the center of the focal point should be considered rather as the sum of the ultrasound waves coming from each point of the emitter surface (a disk of 6.6 mm diameter) and those ultrasound waves are also subject to deflection at each interface layer. However, a simulation taking into account these effects has demonstrated that, for the investigated simple phantom structure, they have a minimal influence on the phase aberration induced by this phantom. The difference between the phase-shift obtained by line integration and obtained by a complete stochastic ray tracing simulation indicates a difference of only $\pm 1^\circ$ for this phantom, which does not significantly influence the refocusing quality.

IV.B. Pressure distribution

Although the phase correction based on the MRI derived acoustic model showed a reduced accuracy compared to the correction based on direct hydrophone measurements, the method allows to recover the similar focal point size with

almost the same pressure level (5%–6% difference) for this aberrator phantom. Compared to the noncorrected experiments, this represents a significant improvement, in particular if the smaller focal point volume at the 50% threshold of the normalized pressure and the higher peak pressure in the focus are considered.

It should be noted that the phase correction does not allow to compensate the elevated attenuation of the polymer aberrator blocks. In principle, a perfect refocusing would need to correct both phase and amplitude for of each transducer element in order to provide an optimal focal point quality. However, the use of an amplitude correction also translates to increased power emissions at locations with increased tissue absorption. This potentially increases the risk of unwanted local overheating, in particular in the near-field of the transducer.

IV.C. Heating efficiency

Since the temperature rise is not only a function of the maximum intensity but also a function of the spatial distribution of the intensity and the thermal diffusion, the heating efficiency obtained in the absence of any phase correction was not as low as expected.

The use of refocusing method increases the maximum intensity (proportional to the square of the pressure) from 49% up to 90% depending on the employed phase correction method. However, the maximum temperature rise observed by MR-thermometry is only 27.7 °C without refocusing and 34–39.2 °C with refocusing. The normalization of those temperature rises corresponds to 71% without refocusing and 87%–100% with refocusing.

This difference of behavior between the maximum intensity and the maximum temperature rise can be explained partially by the fact that the temperature rise is also a function of the spatial distribution of the intensity and the thermal diffusion effect as described by Pennes.[23] Thus, the partial volume effect and the temperature diffusion might have mitigated the effect of the defocusing introduced by the aberrators. For sonications without phase compensation, secondary lobes with almost the same intensity as the main focal point can be expected to have a significant contribution to the temperature increase in the central voxel. However, those secondary lobes also tend to enlarge the heating, which can explain the larger full width at half maximum of the observed temperature distribution.

IV.D. Translation to the clinic

For clinical applications using MR-HIFU for breast cancer therapy, the presented correction approach is potentially beneficial due to the higher precision of the focal point, and thus the delineation of the treatment zone. One major limitation for the translation of this method to a clinical application is the complexity of breast tissue. In general, tumor tissue in the breast usually does not contain fat. In nearby healthy tissue, both water and fat can be expected to be found in the same voxel, and a more complex tissue model than the one presented in this study may be required in order to derive the accurate propagation delay along the beam path of each element. An optimization of the MRI sequence for clinical applications would be required to maximize tissue contrast with a minimal image distortion, especially with respect to the shift of the fat relative to the glandular and tumor tissue.

In addition, it would be necessary to prevent or to compensate for patient motion in clinical applications since the proposed refocusing method requires a localization of tissue types with an accuracy of 1 mm or better. On the other hand, high resolution 3D anatomical MR-images are already routinely obtained directly prior to the HIFU intervention as part of the therapy preplanning.

Although the value of the tissue celerity as a function of breast tissue type has been reported in literature,[21] the tissue celerity can also be expected to be somewhat patient dependent. Therefore, due to the strong dependency of the phase correction on the used celerity values, the requirement of an interindividual quantification of the celerity of each tissue type prior to each treatment session needs to be investigated.

In addition, the tissue celerity also depends on tissue temperature. For most biologic tissues, the sound velocity increases with temperature with about 2.2 m/s/°C for a temperature range up to 50 °C. In contrast, for lipids in interstitial tissue such as breast fat, the sound velocity decreases with temperature with an estimated slope of − 3.1 m/s/°C.[24] The difference of celerity between fatty and glandular tissues increases by a factor 2 from 87 to 174 m/s with a temperature rise of + 16.4 °C. As a consequence, it might also be necessary to take into account the temperature distribution in the used model to process the phase correction.

V. CONCLUSIONS

Although the effectiveness of the proposed correction method is in practice limited by the spatial resolution of the MR images and the accuracy of the tissue celerity quantification, the presented first experiments under realistic conditions showed very encouraging results: An optimal focal point shape allows the increase of the ablation efficiency and to reduce the risk of undesired tissue damage in adjacent areas. The proposed method is noninvasive and compatible with a standard interventional preplanning and thus a step toward optimal treatment efficiency of MR-guided HIFU ablations in heterogeneous tissues such as the human breast. Future work will include an analysis of the required MR resolution and accuracy of the tissue celerity of biological tissue samples.

ACKNOWLEDGMENTS

The authors like thank Erkki Vahala for his invaluable contributions to the stochastic ray tracing method for acoustic field simulation. The authors wish to thank FUS foundation for a supporting grant.

APPENDIX: SIMULATION METHOD

This appendix provides an overview of the method used for all simulations in this work carried out with stochastic ray tracing method[25] used to model acoustic field.

In this approach, the simulation domain is divided into homogeneous subdomains. Each transducer element is treated as a source for a large number of computational phonons. Each phonon has a propagation direction $\vec{d}$, a complex-valued pressure amplitude p, and accumulated travelled distance R. Initially, all phonons are placed at the centers of the transducer elements. The propagation directions are chosen randomly, such that they sample the directivity pattern of the transducer elements. The sampling probability of each pick p_s is recorded and associated with the corresponding phonon.

The computational phonons are propagated through the simulation domain along trajectories computed by ray tracing. The phonon phase and distance are accumulated accordingly. Reflection and refraction at interfaces can be taken into account by splitting a phonon into a reflected phonon and a transmitted phonon, respectively.

Phonon intersections with a region of interest are recorded. As the simulation progresses, an estimate of the pressure field is obtained via stochastic integration. For a phonon i hitting a 2D imaging plane with pixel size $\Delta \times \Delta$, the pressure estimate at the pixel is accumulated through formula (A1)

$$\bar{p}_{\text{pixel}} \rightarrow \bar{p}_{\text{pixel}} + \frac{1}{N_{\text{phonons}}} \cdot \frac{1}{p_{s,i}} \cdot \frac{R_i^2}{\Delta^2 \left| \vec{d}.\vec{n} \right|} \cdot \frac{p_i}{2\pi \cdot R_i}. \qquad \text{(A1)}$$

Here, $\vec{n}$ denotes the normal vector of the imaging plane, and N_{phonons} is the total number of phonons to be simulated. The amplitude p_i and travelled distance R_i are evaluated at the site of the intersection.

[a]Author to whom correspondence should be addressed. Electronic mail: charles.mougenot@philips.com

[1]H. Furusawa, K. Namba, S. Thomasen, F. Akiyama, A. Bendet, C. Tanaka, Y. Yasuda, and H. Nakahara, "Magnetic resonance-guided focused ultrasound surgery of breast cancer: Reliability and effectiveness," J. Am. Coll. Surg. **203**(1), 54–63 (2006).

[2]P. E. Huber, J. W. Jenne, R. Rastert, I. Simiantonakis, H. Sinn, H. Strittmatter, D. Fournier, M. F. Wannenmacher, and J. Debus, "A new noninvasive approach in breast cancer therapy using magnetic resonance imaging-guided focused ultrasound surgery," Cancer Res. **61**(23), 8441–8447 (2001).

[3]C. T. W. Moonen and C. Mougenot, "MRI-Guided Focused Ultrasound, Apparatus for Novel Treatment of Breast Cancer," Philips Research Book Series (Springer, New York), **6**, 183–200 (2006).

[4]E. L. Madsen, J. A. Zagzebski, G. R. Frank, J. F. Greenleaf, and P. L. Carson, "Anthropomorphic breast phantoms for assessing ultrasonic imaging system performance and for training ultrasonographers: Part I," J. Clin. Ultrasound. **10**(2), 67–75 (1982).

[5]E. L. Madsen, J. A. Zagzebski, G. R. Frank, J. F. Greenleaf, and P. L. Carson, "Anthropomorphic breast phantoms for assessing ultrasonic imaging system performance and for training ultrasonographers: Part II," J. Clin. Ultrasound. **10**(3), 91–100 (1982).

[6]L. M. Hinkelman, D. L. Liu, R. C. Waag, Q. Zhu, and B. D. Steinberg, "Measurement and correction of ultrasonic pulse distortion produced by the human breast," J. Acoust. Soc. Am. **97**(3), 1958–1969 (1995).

[7]T. D. Mast, L. M. Hinkelman, L. A. Metlay, M. J. Orr, and R. C. Waag, "Simulation of ultrasonic pulse propagation, distortion, and attenuation in the human chest wall," J. Acoust. Soc. Am. **106**(6), 3665–3677 (1999).

[8]T. D. Mast, "Two- and three-dimensional simulations of ultrasonic propagation through human breast tissue," ARLO **3**(2), 53–58 (2002).

[9]F. J. Fry, "Transkull transmission of an intense focused ultrasonic beam," Ultrasound Med. Biol. **3**(2-3), 179–184 (1977).

[10]J.-L. Thomas and M. Fink, "Ultrasonic beam focusing through tissue inhomogeneities with a time reversal mirror: Application to transskull therapy," IEEE Trans. Ultrason. Ferroelectr. Freq. Control **43**, 1122–1129 (1996).

[11]K. Hynynen and F. A. Jolesz, "Demonstration of potential noninvasive ultrasound brain therapy through an intact skull," Ultrasound Med. Biol. **24**, 275–283 (1998).

[12]K. Hynynen and J. Sun, "Trans-skull ultrasound therapy: The feasibility of using image-derived skull thickness information to correct the phase distortion," IEEE Trans. Ultrason. Ferroelectr. Freq. Control **46**(3), 752–755 (1999).

[13]M. Pernot, J.-F. Aubry, M. Tanter, J.-L. Thomas, and M. Fink, "Experimental validation of finite differences simulations of the ultrasonic wave propagation through the skull," Proc. IEEE Ultrason. Symp. **2**, 1547–1550 (2001).

[14]G. T. Clement and K. Hynynen, "A non-invasive method for focusing ultrasound through the skull," Phys. Med. Biol. **47**, 1219–1236 (2002).

[15]J.-F. Aubry, M. Tanter, M. Pernot, J.-L. Thomas, and M. Fink, "Experimental demonstration of non invasive transskull adaptive focusing based on prior CT scans," J. Acoust. Soc. Am. **113**, 85–93 (2003).

[16]F. Marquet, M. Pernot, J.-F. Aubry, G. Montaldo, L. Marsac, M. Tanter, and M. Fink, "Non-invasive transcranial ultrasound therapy based on a 3D CT scan: Protocol validation and in vitro results," Phys. Med. Biol. **54**(9), 2597–2613 (2009).

[17]G. Salahura, J. C. Tillett, L. A. Metlay, and R. C. Waag, "Large-scale propagation of ultrasound in a 3-D breast model based on high-resolution MRI data," IEEE Trans. Biomed. Eng. **57**(6), 1273–84 (2010).

[18]E. Herbert, M. Pernot, G. Montaldo, M. Fink, and M. Tanter, "Energy-based adaptive focusing of waves: Application to noninvasive aberration correction of ultrasonic wavefields," IEEE Trans. Ultrason. Ferroelectr. Freq. Control **56**(11), 2388–2399 (2009).

[19]Y. Hertzberg, A. Volovick, Y. Zur, Y. Medan, S. Vitek, and G. Navona, "Ultrasound focusing using magnetic resonance acoustic radiation force imaging: Application to ultrasound transcranial therapy," Med. Phys. **37**(6), 2934–2942 (2010).

[20]B. Larrat, M. Pernot, G. Montaldo, M. Fink, and M. Tanter, "MR-guided adaptive focusing of ultrasound," IEEE Trans. Ultrason. Ferroelectr. Freq. Control **57**(8), 1734–1737 (2010).

[21]A. L. Scherzinger, R. A. Belgam, P. L. Carson, C. R. Meyer, J. V. Sutherland, F. L. Bookstein, and T. M. Silver, "Assessment of ultrasonic computed tomography in symptomatic breast patients by discriminant analysis," Ultrasound Med. Biol. **15**(1), 21–28 (1989).

[22]W. E. Lorensen and H. E. Cline, "Marching cubes: A high resolution 3D surface construction algorithm," Comput. Graph. **21**(4), 163–169 (1987).

[23]H. H. Pennes, "Analysis of tissue and arterial blood temperatures in the resting human forearm," J. Appl. Physiol. **1**, 93–122 (1948).

[24]F. A. Duck, *Physical Properties of Tissue—A Comprehensive Reference Book, Acoustic Properties* (Academic Press Limited, London, Canada, 1990), Chap. 4.

[25]R. L. Cook, T. Porter, and L. Carpenter, "Distributed ray tracing," Comput. Graph. **18**(3), 137–145 (1984).